COBEM 99
XV Congresso Brasileiro de Engenharia Mecânica
15th Brazilian Congress of Mechanical Engineering
22 - 26 de Novembro de 1999 / November 22 - 26, 1999 Águas de Lindóia, São Paulo,

NATURAL CONVECTION IN A POROUS CAVITY USING THE GENERALIZED MODEL WITH UNIFORM POROSITY

Jesus Marlinaldo de Medeiros
Escola Técnica Federal de Sergipe/UNED
49056-260 – Lagarto – SE - Brasil
Francisco Marcondes
Universidade Federal da Paraíba, Departamento de Engenharia Mecânica
Cx. P. 10.069 – 58109-970 – Campina Grande – PB - Brasil
José Maurício Gurgel
Universidade Federal da Paraíba, Departamento de Tecnologia Mecânica
Cx. P. 5.115 – 58059-900 – João Pessoa – PB - Brasil

Abstract. *This study presents a numerical investigation of convective heat transfer in a rectangular porous cavity using the generalized model with uniform porosity based on the Brinkman and Forchheimer models in Navier-Stokes equations which are applied to an interval involving Darcian and non-Darcian regimes. Results are presented through temperature and vertical velocity profiles as well as the average Nusselt number calculated in the vertical walls of the cavity. These results were compared with other numerical studies , verifying a good agreement. It was also proposed a correlation in order to calculate the average Nusselt number at five dimensionless parameters, such as: aspect ratio, Rayleigh number, Darcy number, Prandtl number and the porosity. It was observed a discrepancy about 30% in relation to the simulated results.*

Key–words*: Natural convection,* porous *medium, uniform porosity, Darcian and non-Darcian regimes.*

1. INTRODUCTION

In the last three decades the analysis of the thermal field in a porous medium has attracted a great deal of attention because of the necessity to know the thermal-hydrodynamic behavior which is involved in geophysical systems, storage and drying of grains, oil reservoir engineering, besides thermal insulation projects. The wide range of researches that were developed in the heat transfer area in a porous medium, used fundamentally the approximations based on Darcy's law. Nevertheless, when the porous medium permeability is high, Darcy's model doesn't present satisfactory results when compared with experimental data. This discrepancy in theoretical results with experimental data was initially analyzed by Cheng (1978), in order to investigate the thermal behavior and its applications in geothermal systems.

By virtue of this divergence, several efforts were accomplished to include inertial and viscous terms in momentum equations with the purpose of examining its effects, to develop a mathematical model which should be reasonably accurate and in which experimental data are corroborated. Both inertial and viscous terms were added forming , thus, the non-Darcian model that lacked of a formalism which could legitimate it. Finally, Slattery (1978) solved the problem through the development of medium equations starting from mechanical of continuous equations, developing a theorem to associate averages of gradients and gradients of averages. As a result, the Darcy's model , which was perfected by Brinkman and Forchheimer, and more accurate models proposed by Vafai & Tien (1981), appeared using the Local Volume Averaging Technique given by Nithiarasu et al. (1979) , that are originated from a balance of properties in a control volume. Although these more complete models originate themselves from different principles, they are equivalent, because they result in the same momentum equations, including the Forchheimer and Brinkman terms. Medeiros et al. (1998) investigated numerically the heat transfer by natural convection, in a quadratic porous and saturated cavity, based on non- Darcian regime, using the generalized model with the Brinkman and Forchheimer terms in the Navier-Stokes equations, considering an uniform porosity and then they conclude that the applied method agrees very well with those methods referred in literature.

This research intends to validate the mathematical model as well as the numerical method that has been used in a rectangular cavity at several aspect ratio and to present results through temperature and velocity profiles, and the average Nusselt number (which is calculated in the vertical walls of the cavity).It was also proposed a correlation in order to calculate the above-mentioned average Nusselt number, considering uniform porosity , in function of five dimensionless parameters: aspect ratio, Rayleigh number, Darcy number, Prandtl number and the porosity.

2. MATHEMATICAL FORMULATION

The problem in relation to the heat transfer by natural convection in a porous rectangular cavity, as shown in Fig. 1, was numerically simulated using the generalized model based on the Brinkman's and Forchheimer's terms, in the Navier-Stokes equations proposed by Nithiarasu et al. (1997). This model is obtained through the balance of properties assuming, an isotropic homogeneous and saturated porous medium by an incompressible fluid, two-dimensional and laminar flow, use of Boussinesq approach in the modeling of the buoyancy term, fluid and the solid matrix in local thermal equilibrium, and there is not any change of the phase of the fluid.

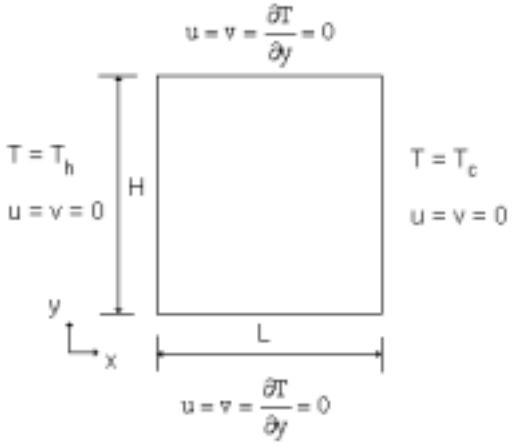

Figure 1 – Geometry and boundary conditions of the problem

The system of equations for a formulation of the problem in Cartesian coordinates can be written as:

$$\frac{\partial}{\partial x}(\rho_f\ u)+\frac{\partial}{\partial y}(\rho_f\ v)=0 \tag{1}$$

$$\frac{\partial}{\partial t}(\rho_f u)+\frac{\partial}{\partial x}\left(\frac{\rho_f uu}{\varepsilon}\right)+\frac{\partial}{\partial y}\left(\frac{\rho_f vu}{\varepsilon}\right)=-\frac{\partial p}{\partial x}+\frac{\partial}{\partial x}\left(\mu_f\frac{\partial u}{\partial x}\right)+\frac{\partial}{\partial y}\left(\mu_f\frac{\partial u}{\partial y}\right) -\frac{\mu_f\varepsilon}{K}u-\frac{1{,}75\rho_f\left|\vec{V}\right|}{\sqrt{150K\varepsilon}}u \tag{2}$$

$$\frac{\partial}{\partial t}(\rho_f v)+\frac{\partial}{\partial x}\left(\frac{\rho_f uv}{\varepsilon}\right)+\frac{\partial}{\partial y}\left(\frac{\rho_f vv}{\varepsilon}\right)=-\frac{\partial p}{\partial y}+\frac{\partial}{\partial x}\left(\mu_f\frac{\partial v}{\partial x}\right)+\frac{\partial}{\partial y}\left(\mu_f\frac{\partial v}{\partial y}\right) +\rho_f\beta_f g\varepsilon(T-T_c)-\frac{\mu_f\varepsilon}{K}v-\frac{1{,}75\rho_f}{\sqrt{150K\varepsilon}}\left|\vec{V}\right|v \tag{3}$$

$$(\rho c_p)_m\frac{\partial T}{\partial t}+(\rho c_p)_f\left(\frac{\partial}{\partial x}(uT)+\frac{\partial}{\partial y}(vT)\right)=\frac{\partial}{\partial x}\left(\kappa_m\frac{\partial T}{\partial x}\right)+\frac{\partial}{\partial y}\left(\kappa_m\frac{\partial T}{\partial y}\right) \tag{4}$$

where ε and K are respectively the porosity and the absolute permeability related to the porous medium and ρ_f, μ_f, c_{pf}, and β_f are the specific mass, viscosity, specific heat at constant pressure and the thermal expansion coefficient of the fluid. In addition, k_m, the thermal conductivity of the saturated porous medium, is mathematical function of the porosity medium and also of the thermal conductivity ratio between the solid and the liquid. While u, v, p, T and g are vector velocity Cartesian components ,the medium pressure, the temperature and the gravity acceleration, respectively. The last two terms of Eqs. (2) and (3) represent the Brinkman and Forchheimer terms.

The equations (1)-(4) can be non-dimensioned using the following parameters:

$$X=\frac{x}{L}\quad Y=\frac{y}{L}\quad U=\frac{uL}{\alpha_f}\quad V=\frac{vL}{\alpha_f}\quad \alpha_f=\frac{k_f}{(\rho c_p)_f}\quad P=\frac{pL^2}{\rho_f\alpha_f^2}\quad \theta=\frac{T-T_c}{T_h-T_c} \tag{5}$$

$$R_K=\frac{k_m}{k_f}\quad Ra=\frac{g\beta_f\Delta TL^3}{\alpha_f\nu_f}\quad Da=\frac{K}{L^2}\quad Pr=\frac{\nu_f}{\alpha_f}\quad \sigma=\frac{(\rho c_p)_m}{(\rho c_p)_f}\quad \tau=\frac{t\alpha_f}{L^2}\quad A=\frac{H}{L} \tag{6}$$

where α_f, k_f, R_k, Ra, Da, Pr, σ and A are respectively the thermal diffusivity of the fluid, the thermal conductivity of the fluid, the conductivity ration between the medium and the liquid phase, Rayleigh number, Darcy number, Prandlt number, the thermal capacity ratio and the aspect ratio of cavity. In the present work, the thermal properties of the fluid-porous matrix were considered unitary ((σ =1, k_m = k_f), that is to say the effects of the conductivity ratio as well as the thermal capacity ratio were not taken into consideration. Using the dimensionless parameters of Equations (5) – (6) , the Eqs. (1)-(4) formed the following set of dimensionless equations:

$$\frac{\partial U}{\partial X}+\frac{\partial V}{\partial Y}=0 \tag{7}$$

$$\frac{\partial U}{\partial \tau}+\frac{\partial}{\partial X}\left(\frac{UU}{\varepsilon}\right)+\frac{\partial}{\partial Y}\left(\frac{VU}{\varepsilon}\right)=-\frac{\partial P}{\partial X}+\frac{\partial}{\partial X}\left(Pr\frac{\partial U}{\partial X}\right)+\frac{\partial}{\partial Y}\left(Pr\frac{\partial U}{\partial Y}\right)$$
$$-\frac{1{,}75}{\sqrt{150\,Da\,\varepsilon}}\left(U^2+V^2\right)^{1/2}U-\frac{Pr}{Da}\varepsilon\,U \tag{8}$$

$$\frac{\partial V}{\partial \tau}+\frac{\partial}{\partial X}\left(\frac{UV}{\varepsilon}\right)+\frac{\partial}{\partial Y}\left(\frac{VV}{\varepsilon}\right)=-\frac{\partial P}{\partial Y}+\frac{\partial}{\partial X}\left(Pr\frac{\partial V}{\partial X}\right)+\frac{\partial}{\partial Y}\left(Pr\frac{\partial V}{\partial Y}\right)$$
$$+Pr\,Ra\,\varepsilon\,\theta-\frac{1{,}75}{\sqrt{150\,Da\,\varepsilon}}\left(U^2+V^2\right)^{1/2}V-\frac{Pr}{Da}\varepsilon\,V \tag{9}$$

$$\sigma\frac{\partial \theta}{\partial \tau}+\frac{\partial}{\partial X}(U\theta)+\frac{\partial}{\partial Y}(V\theta)=\frac{\partial}{\partial X}\left(R_k\frac{\partial \theta}{\partial X}\right)+\frac{\partial}{\partial Y}\left(R_k\frac{\partial \theta}{\partial Y}\right) \tag{10}$$

In equations (7)-(10), the following dimensionless boundary conditions were employed:

$$U=V=\frac{\partial \theta}{\partial Y}=0 \quad \text{at} \quad Y=0 \text{ and } Y=A \tag{11}$$

$$U=V=0 \quad \text{at} \quad X=0 \text{ and } X=1 \tag{12}$$

$$\theta=1 \text{ at } X=0 \text{ and } \theta=0 \text{ at } X=1 \tag{13}$$

3. NUMERICAL PROCEDURE

The proposed problem in this research forms a system of nonlinear elliptical differential equations composed by the continuity equation, momentum equations in directions *x* and *y* and finally the energy equation. These equations were discretized based on the Finite Volume Method given by Patankar (1980) and Maliska (1995), using the staggered grid of variables. In this grid, the pressure and temperature are kept in the center of the control volume, while the control volumes for the velocities are located in the faces of the volumes of pressure. In order to evaluate the property and its gradients in the surface of each control volume, it was used the interpolation scheme WUDS (Weighted Upstream Differencing Scheme). On the other hand, to solve the problem of velocity-pressure coupling, it was used the PRIME(Pressure Implicit Momentum Explicit), Maliska (1995).

The iterative cycle, to solve the velocity-pressure coupling, obeyed the following stages: a) Estimating the U, V and θ variables. b) Calculating the momentum equations coefficients. c) Calculating the $\hat{U}_e, \hat{U}_w, \hat{V}_n e \hat{V}_s$ velocities in all of the interfaces of the elementary volume to the pressure. These velocities are not obtained from the solution of linear systems, but throughout the momentum equation and they contain all of the terms except for the pressure ones. d) Solving the linear system at P. e) Correcting the velocities, by using the correction equations, so that these equations can satisfy the mass conservation. f) Solving the linear system at θ and after returning to the item b), iterating until the convergence.

In order to find a solution to the P and θ linear systems, GMRES, given by Saad et al (1986),was considered. It is also preconditioned on the right with an incomplete factoring ILU(1) Marcondes et al(1995). As a criterion of stopping in the solution of these linear systems, it was established that $||r||/||r_0||<10^{-4}$, where $||r||$ is the second residue vectorial pattern and $||r_0||$ is the second initial residue vectorial pattern. In fact, one of the reasons for employing the GMRES approach is due to the slow convergence or the global non-convergence of the problem. Because of this, TDMA was used to solve these above-mentioned linear systems.

As a global convergence criterion, it was proposed the following approach in U and V, given by Maliska (1995): $\left(\phi_i^{n+1} - \phi_i^n\right) \Big/ \left|\phi_{max} - \phi_{min}\right| \leq 10^{-5}$. Where$|\phi_{max}$-$\phi_{min}|$ represents the maximum variation in U or V which was achieved in the –iteration n. When in some point, this equation was not verified , a new iteration was requested.

In this paper, it was used a mesh with exponential variation close to the walls, where there are more accentuated gradients. For more detailed information, see Anderson et al.(1984).A staggered grid of variables and the computational mesh used in the simulations are presented in Fig. 2. A mesh refinement study was accomplished and it was found independent results of the mesh from 61x61 volumes.

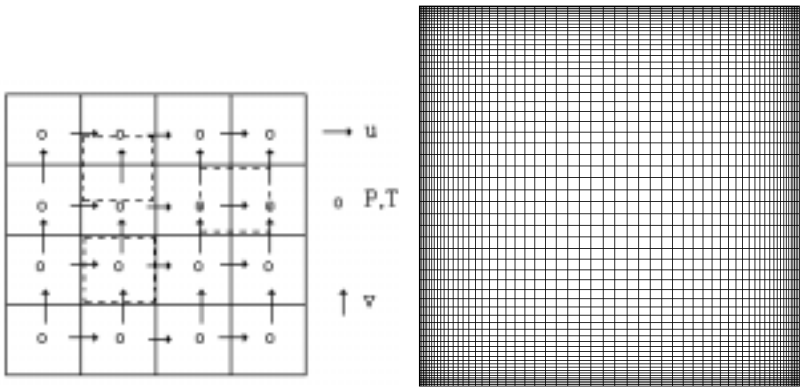

Figure 2 – Grid of variables and computational mesh (61 x 61)

4. RESULTS AND DISCUSSIONS

Initially , the generalized model was tested for being applied in a spectrum interval, involving from the Darcian model (Da= 10^{-7}) until the non-Darcian regime (Da= 10^{-6}). The modified Rayleigh number (Ra_m=Ra_xDa) from 10 to 1000, in the Darcian regime, and from 100 to 5000 in the non-Darcian regime. In fact, this difference between the two intervals above-mentioned is merely to compare with other researches. For the whole cases, the following values were considered for the dimensionless ones: : Pr =1 and Pr=0,01, σ =1, R_k = 1, $1 \leq A \leq 10$ and ε = 0,4, 0,6 e 0,9.

The average Nusselt number, $\overline{Nu}_H$, in the cold and hot walls, was calculated by:

$$\overline{Nu}_H = \frac{\overline{hH}}{k} = -\int_0^A \left.\frac{\partial\theta}{\partial X}\right|_{X=0 \text{ ou } X=1} dY \qquad (14)$$

4.1 Numerical Validation

The table 1 shows the average Nusselt number on the left wall at Darcian regime in comparison to other mentioned researches in literature. The Walker & Homsy (1978) works and Trevisan & Bejan(1986) studies employed the Darcy's model. On the other hand, Nithiarasu et al. (1996) used the generalized model based on Brinkman & Forchhemier terms and Lauriat and Prasad (1989) made use of a similar model to the above-mentioned generalized model. It is interesting to note that with exception of Trevisan & Bejan study (1996), at Ra_m=1000, the results, that were obtained in this present research , show a good agreement in relation to the results which were achieved through different physical model, as shown in Tab. 1:

Table 1 – A comparison of the model in Darcian regime ($Da=10^{-7}$,Pr=1,A=1 and $\varepsilon = 0,4$)

Nu_H left face					
Ra_m	Walker & Homsy (1978)	Lauriat & Prasad (1989)	Trevisan & Bejan (1986)	Nithiarasu *et al*. (1996)	Present research
10	-	1,07	-	1,08	1,08
50	1,98	-	2,02	1,96	1,98
100	3,09	3,09	3,27	3,02	3,10
500	8,40	-	-	8,38	8,89
1000	12,49	13,41	18,38	12,51	13,38

Table 2 presents the average Nusselt number on the left wall at non-Darcian approach in comparison to Nithiarasu et al. (1997). Note that there is also a good agreement between the results in a non-Darcian regime, for different Darcy's values, and the porosity. In spite of not representing in a appropriate way a porous medium, the ε= 0,9 case was simulated only to effect of validation of the results with those studied widely in literature.

Tabela 2 - A comparison of the model in non-Darcian regime (Pr=1 and A=1).

$\overline{Nu}_H$ left face							
Ra_m	Da	ε=0,4		ε=0,6		ε=0,9	
		Nithiarasu *et al.* (1997)	Present research	Nithiarasu *et al.* (1997)	Present research	Nithiarasu *et al.* (1997)	Present research
100	10^{-6}	2,97	3,05	3,00	3,07	3,00	3,08
1000	10^{-6}	11,46	12,10	11,79	12,57	12,01	12,90
5000	10^{-6}	23,09	24,74	25,37	26,77	26,91	28,49
100	10^{-4}	2,55	2,60	2,72	2,70	2,74	2,79
1000	10^{-4}	7,81	7,76	8,18	8,56	9,20	9,31
5000	10^{-4}	13,82	13,60	15,57	15,34	16,77	17,14
100	10^{-2}	1,41	1,36	1,53	1,49	1,64	1,63
1000	10^{-2}	2,98	2,99	3,56	3,44	3,91	3,92
5000	10^{-2}	4,99	4,99	5,74	5,76	6,70	6,59

4.2 Analysis of Results

Figure 3 shows the temperature and vertical velocities profiles, respectively in a average horizontal line of the cavity, at Ra_m=1000, and it still shows that the Darcy regime varies from 10^{-7} to10^{-2}, and ε=0,4.It should be noted that for $Da \leq 10^{-4}$, the temperature profiles are

very similar. In these cases, the same thermal boundary layer occurs approximately near the walls and the heat transfer in the central area of the cavity practically occurs by diffusion. However, at $Da=10^{-2}$, the thickne--ss of the thermal boundary layer is very different from the others ones and it also happens a change in the central area. The temperature profile has a tendency to present the thermal inversion effect. In fact, the fluid, which is contained in the cavity, transports energy from the hot wall to the cold one and it flows close to the walls, but when the medium permeability increases, these fluid begins to interact in the process. On the other hand, the thermal inversion happens because the flowing fluid in the bottom portion of the cavity, by approaching to the hot wall, loses heat to the central area of the cavity, and this makes the temperature increases. The important point to be noted here is that due to Pr=1, the thickness of the thermal and kinetics boundary layers is approximately the same.

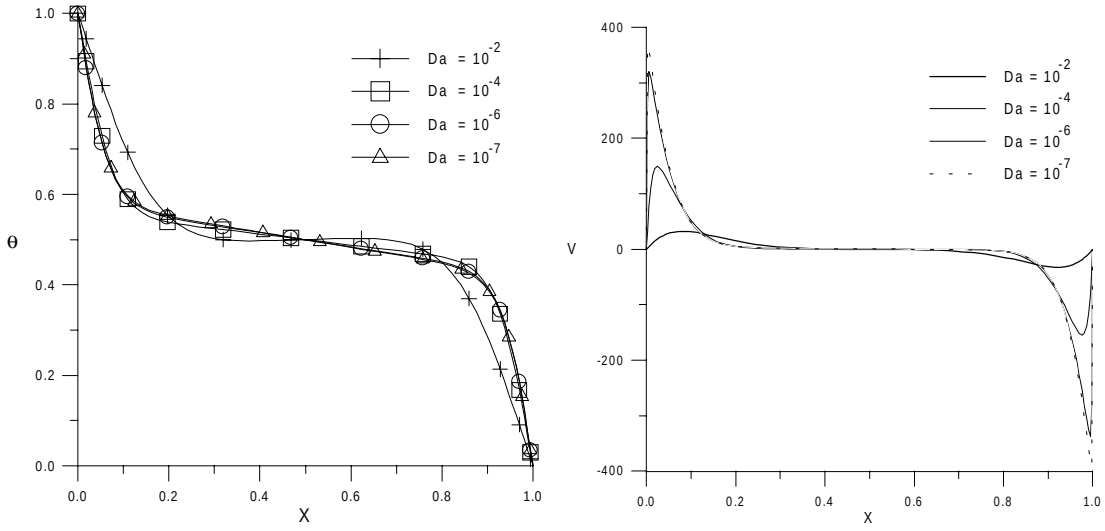

Figure 3 – Temperature and vertical velocity profiles in the averaging horizontal line at Ra_m=1000, Pr=1,A=1 and ε = 0,4.

It is seen from figure 4 that the temperature and vertical velocities profiles in the averaging horizontal line of the cavity for $Da=10^{-7}$, at Ra_m varying from 100 to 5000 and ε=0,4. At Ra_m=100, the temperature approaches to a conductive behavior and at $Ra_m \geq 500$, the profiles are quite altered by the convection. Observe that practically the whole flow occurs near the walls, whereas the whole fluid in the central area remains stagnant. Evidently, this happens due to the high speed gradient close to the vertical walls. An abrupt variation of the velocities profiles close to the walls is observed, showing thus, a similar situation in the sliding condition.

In figure 5, it can noted that the temperature and vertical velocities profiles respectively in the averaging horizontal line of the cavity for $Da=10^{-2}$, at Ra_m varying from 100 to 5000 and ε=0,4. It is observed a similar behavior to that described in the previous paragraph, however, verifying the decrease of the velocity gradient close to the vertical walls, due to the increase of medium permeability. In this case, it is interesting to note that the velocity gradients are plenty of inferior to every simulated numbers Ra_m. It is still noticed the appearance of the thermal inversion effect at Ra_m = 5000.

The figure 6 presents the average Nusselt number for aspect ratio (A) equals to 1,5 and 10, Prandtl number 0,01 and 1, and $Da=10^{-6}$ and 10^{-2} in a interval Ra_m from 100 to 5000. It is verified that the aspect ratio increase or Prandtl decrease cause the average Nusselt number increase through the cavity in both of studied cases.

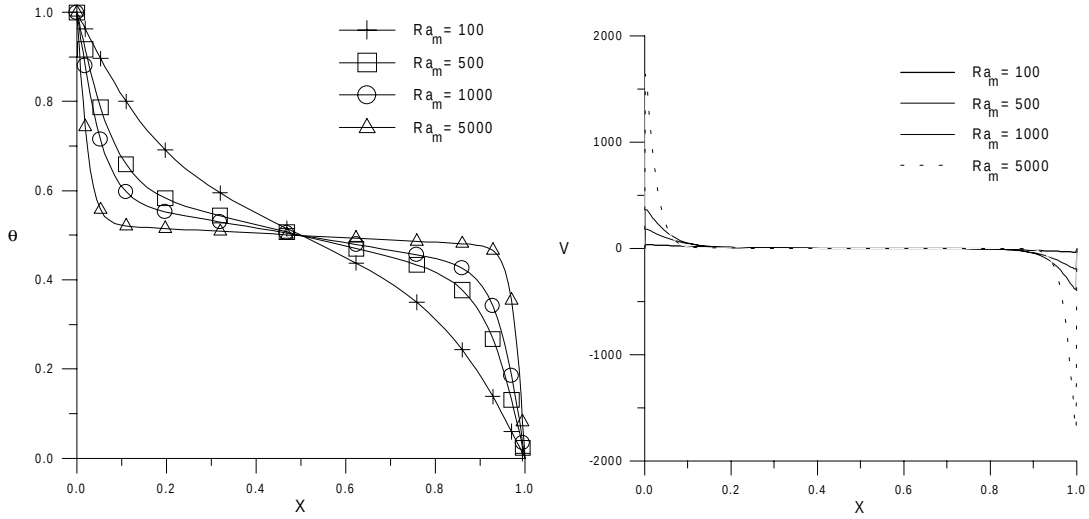

Figure 4 – Temperature and vertical velocity profiles in the average horizontal line at $Da=10^{-7}$, Pr=1,A=1 and ε = 0,4.

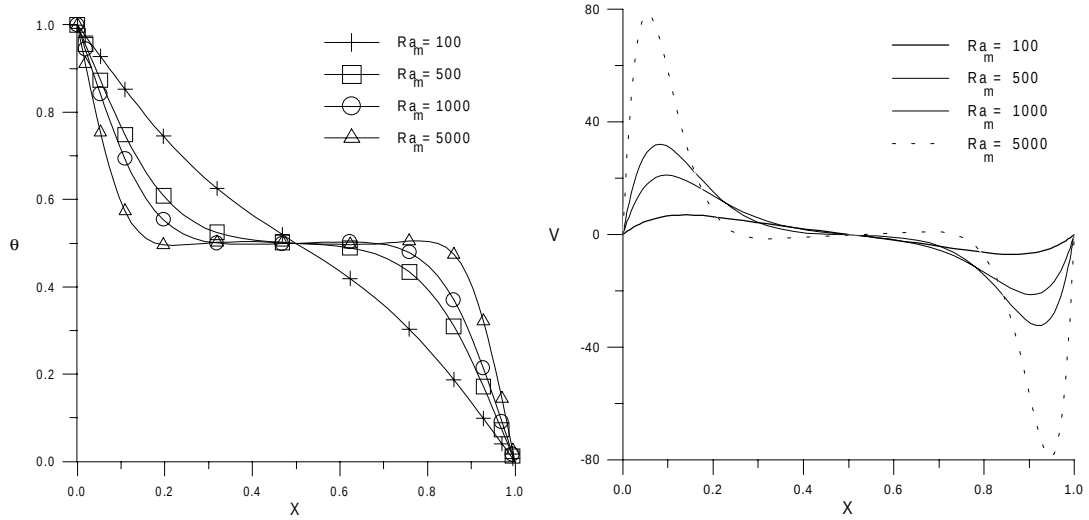

Figure 5 – Temperature and vertical velocity profiles in the average horizontal line at $Da=10^{-2}$, Pr=1,A=1 and ε = 0,4.

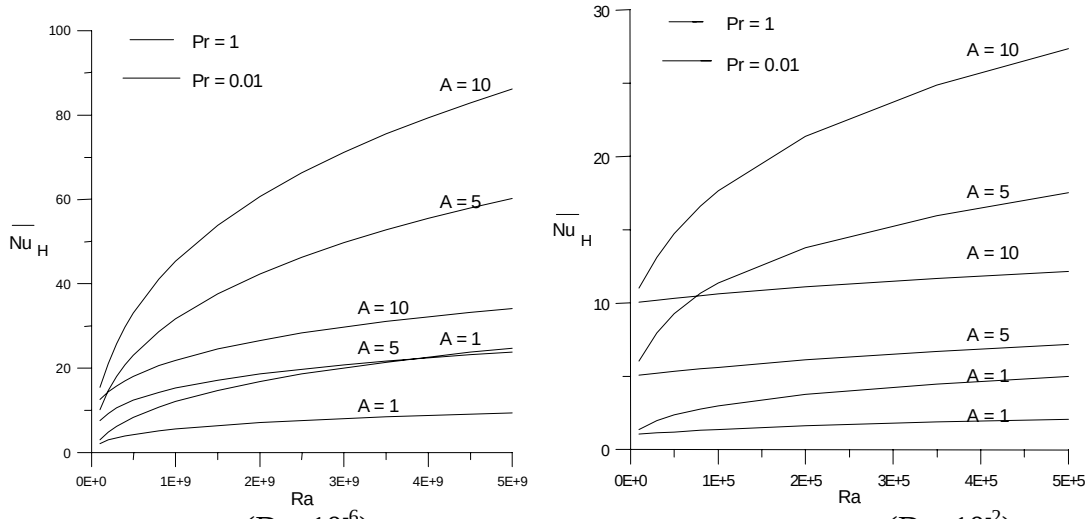

($Da=10^{-6}$) ($Da=10^{-2}$)

Figure 6 - Average Nusselt number at Ra_m = 100 to 5000, A=1, 5, 10, Pr=1, 0,01 and ε=0,4

4.3 Proposed correlation

In order to group the several simulated results presented in fig. (6), it was suggested a correlation at $\overline{Nu}_H = f(A, Ra, Da, Pr, \varepsilon)$, which is defined as:

$$\overline{Nu}_H = a\, A^b Ra^c Da^d Pr^e \varepsilon^f \tag{15}$$

The domain that guided the simulations was the following: aspect ratio ($1 \leq A \leq 10$), ($5x10^6 \leq Ra \leq 5x10^9$), Darcy ($10^{-6} \leq Da \leq 10^{-4}$), Prandtl (Pr=0,01 e 1) and porosity ($0,4 \leq \varepsilon \leq 0,9$). Thus, 264 simulations were accomplished at an interval Ra_m that is established from 500 to 5000. With the simulation values, it was obtained the following correlation for the average Nusselt number in the cavity, for the overall analyzed domain:

$$\overline{Nu}_H = 0.202\, A^{4/7} Ra^{3/8} Da^{1/4} Pr^{1/6} \varepsilon^{2/9} \tag{16}$$

Figure 7 presents the simulated values versus Eq. (16), containing the overall above-mentioned domain. A discrepancy is verified among the simulated results and results calculated through Eq. (16), which is inferior at 30%.

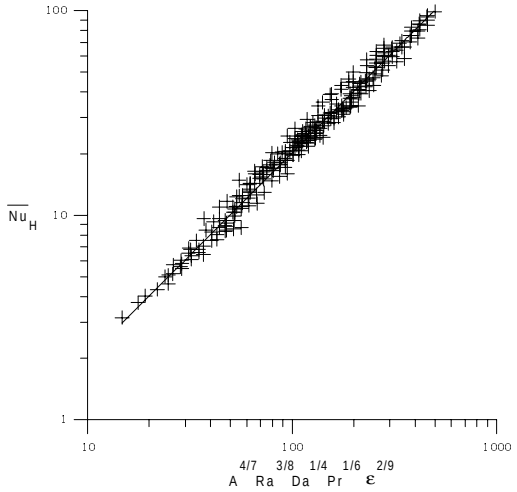

Figure 7 – correlation at Nusselt number, $\overline{Nu}_H = f(A, Ra, Da, Pr, \varepsilon)$

5. CONCLUDING REMARKS

In this analyses , it was observed that the proposed problem using the generalized model with uniform porosity obtained a good performance in relation to other researches. It was also noted the influence of the permeability in the fluid flow and consequently in the heat transfer rate, in the cavity through the temperature and vertical velocity profiles. It was proposed a correlation for the average Nusselt number in function of five dimensionless parameters, such as: aspect ratio, Rayleigh, Darcy and Prandtl numbers and the porosity. Thus, it was observed a discrepancy about 30% among the simulated results and the established correlation. This can be statistically attributed to the small number of simulated results, opposite to the number of so many involved parameters or even to parameters that will be analyzed later on a scaling analysis, in order to define the dominant parameters of the problem.

6. REFERENCES

Anderson, D. A., Tannehill, J. C. & Pletcher, R. H., 1984, Computacional Fluid Mechanics and Heat Transfer, Hemisphere Pub. Corporation.

Cheng. P., 1978, Heat transfer in geothermal systems, Advances in Heat Transfer, , vol. 4, pp.1-105.

Lauriat, G. & Prasad, V., 1989, Non-Darcian effects natural convection in a vertical porous enclosure, Int. J. Heat & Mass Transfer, Vol.32, pp 2135-2148.

Maliska, C. R., 1995, Transferência de Calor e Mecânica dos Fluidos Computacional, Editora LTC, Rio de Janeiro.

Marcondes, F., Zambaldi, M. C. & Maliska, C. R., 1995, Comparison of Stationary Methods and GMRES in Petroleum Reservoir Simulation Using non-Structured Voronoi's Mesh, RBCM, XVII, pp. 360-372. (in Portuguese).

Medeiros, J. M., Marcondes, F. & Gurgel, J. M., 1998, Natural Convection in a Retangular Porous Cavity in Non-Darcian Model, VII ENCIT, Rio de Janeiro, RJ BRASIL, pp 1260-1265. (in Portuguese).

Nithiarasu, P., Seetharamu, K. N. & Sundararajan, T., 1996, Double-Diffusive Natural convective in enclosure filled with fluid-saturated porous medium: a generalized non-darcy approach, Numerical Heat Transfer, Part A, Vol.30, pp 413-426.

Nithiarasu, P., Seetharamu, K. N. & Sundararajan, T., 1997, Natural convective heat transfer in a fluid saturated variable porosity medium, Int. J. Heat & Mass Transfer, Vol.40, pp 3955-3967.

Patankar,S.V., 1980, Numerical Heat Transfer and Fluid Flow, Hemisphere, New York.

Saad, Y. & Schultz, M. H., 1986, GMRES: A Generalized Minimal Residual Algorthm for Solving Nonsymmetric Linear Sustems**,** SIAM J. Sci. Stat. Compt., Vol. 7, pp. 857-869.

Slattery, J. C., 1978, Momentum, Energy and Mass Transfer Continua, Krieger, New York.

Trevisan, O. V. & Bejan. A., 1986, Mass and Heat Transfer by Natural Convection in a Vertical Slot Filled with Porous Medium, Int. J. Heat & Mass Transfer, Vol.29, pp 403-415.

Vafai, K & Tien, C. L., 1981, Boundary and inertia effects on flow and heat transfer in porous media, Int. J. Heat & Mass Transfer, Vol.24, pp 195-204.

Walker, K. L. & Homsy, G. M., 1978,Convection in a porous cavity, Journal of Fluid Mechanics, Vol. 87, pp. 449-474.